10 早期再分極症候群

早期再分極（early repolarization）症候群またはJ波症候群は，Haïssaguerre らが2008年に，下側壁誘導における下側壁早期再分極症候群という概念をNew England Journal of Medicine誌に発表して以来[1]，急速に注目を集めている突然死疾患である．本疾患は特発性心室細動（idiopathic ventricular fibrillation: IVF）の1種であるBrugada症候群に類似しているが，Brugada症候群がV_1〜V_3誘導でのcoved型，またはsaddle-back型という特異的なST上昇を示すのに対し，主としてⅡ，Ⅲ，aV_F誘導またはⅠ，aV_L，V_4〜V_6誘導での1 mm以上の波高のJ波（notch or slur）とそれに続くST上昇を特徴とする．一方，従来からV_4〜V_6誘導での早期再分極波形が若年男性に多く存在することも知られており，これらは予後が良好と報告されていた．現時点で，下側壁の早期再分極症候群はその有病率，発症率，後ろ向き予後が判明しつつある段階であるが，発症機序，遺伝的背景は解明途中であり，前向きの予後，予後予測因子は未解明である．本項では，現時点で判明している下側壁早期再分極症候群の病態について述べる．

A 心電図所見

Haïssaguerre の定義では，下側壁の早期再分極症候群とは前述のように，側壁（Ⅰ，aV_L，V_4〜V_6）または下壁（Ⅱ，Ⅲ，aV_F）誘導のうち，2誘導以上で1 mm以上の高さのJ波とST上昇が認められる症例を指す（図1）．Haïssaguerre らは早期

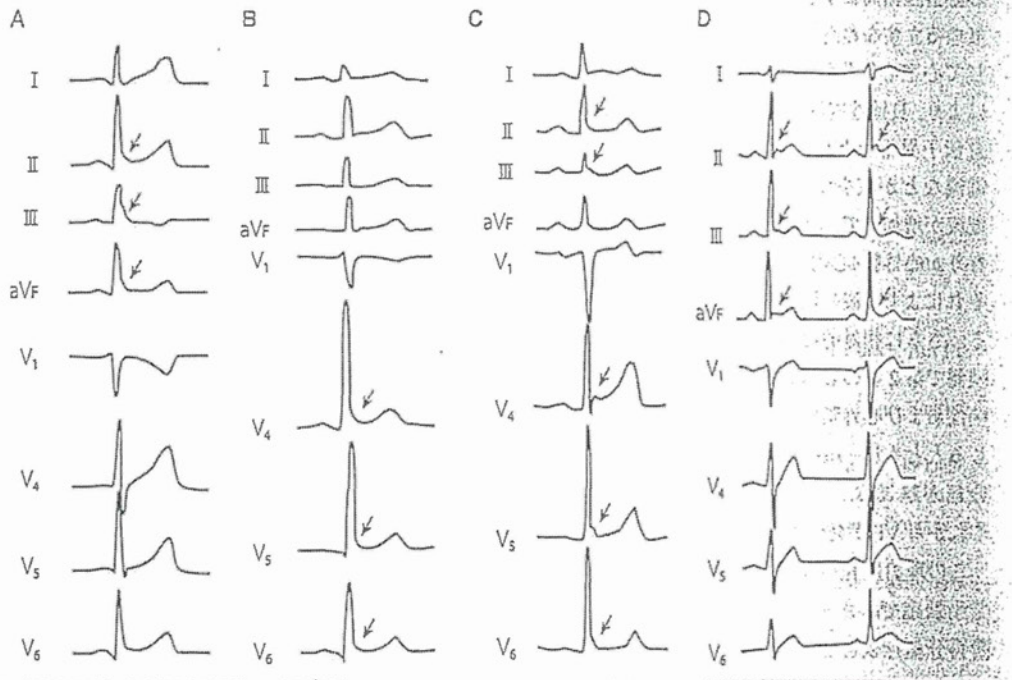

図1 下側壁早期再分極症候群の心電図
矢印はnotchまたはslurのあるJ波を示す．
（文献1より引用）

再分極症候群から典型的なBrugada症候群，すなわちtype 1（coved型）のBrugada症候群を除外しているが，type 2，type 3などsaddle-back型のBrugada波形を有する症例は除外していない．このため，下側壁の早期再分極症候群には前壁の早期再分極を合併するものが一部含まれると考えたほうがよい．

J波はBrugada波形と同様に，記録時期により形状や高さが異なる，または消失することもあるので，できるだけ多くの心電図で評価する必要がある．

B J波と心室細動発生機序

J波の類似波形は低体温時にみられるOsborn波として知られているが，それ以前の1930年代から，J波は正常亜型の波形として健常成人の数%，とくに若年男女にみられると報告されていた．一方，J波の存在する例でVFが生じることは1984年頃から報告されはじめ，Aizawaらが下壁誘導や側壁誘導でJ波の存在する複数例を報告している[2]．

このJ波とVFの機序に関しては，Antzelevitchらが動脈灌流心筋切片を用いたモデルで，心内膜側と心外膜側間に生じる貫壁性電位勾配の差で説明している．すなわち，活動電位第1相において，主として心室心外膜側に生じる一過性外向き電流（I_{to}）により，貫壁性電位勾配が生じてJ波が出現するが，遺伝子異常などにより，内向きのNa^+電流やCa^{2+}電流などが減少すると，I_{to}を含む相対的な外向き電流が増加して，活動電位第1相のnotchが大きくなり，心外膜-心内膜間に大きな電位勾配が生じる．それによりJ波の増大に引き続いてST上昇が起こる．さらに相対的な外向き電流が増加すると，心外膜側で第2相のdome形成が遅延または消失し，貫壁性および心外膜層内で再分極時間のばらつきが生じるとともに，domeの消失した心筋において再脱分極が起こる．これはphase 2 reentryと呼ばれ，これからVFが発生するとされている．

この理論はBrugada症候群におけるJ波とVFの発生機序でもあり，このためAntzelevitchらは早期再分極症候群とBrugada症候群が一連の疾患であるとして，早期再分極症候群を4つのタイプに分類している．すなわち①側壁誘導（I，V_4〜V_6）にのみJ波が存在するものを早期再分極（ERS）type 1，②下壁誘導（II，III，aV_F）または下側壁誘導に存在するものをERS type 2，③下壁と側壁，および前壁の広範囲誘導（global leads）に存在するものをERS type 3，そして④Brugada症候群とし，早期再分極症候群では①〜③の順で危険性が増すとしている[3]．

一方，J波が真に再分極の波形なのかを疑問視する報告もある．Surawiczらは，種々の論文で引用された早期再分極波形からJ波の時相を検討すると，J波はR波の一部に過ぎない可能性があり，再分極の波形とは断言できないと述べている．またAbeらは加算平均心電図の検討から，J波は再分極異常よりも脱分極異常に由来するのではないかと述べている．Kawataらも下側壁誘導のJ波がNa^+チャネル遮断薬で減高することから，下側壁誘導のJ波はBrugada症候群に認められる前壁誘導のJ波とは機序が異なる可能性を指摘している[4]．

この他，J波は急性心筋虚血，肥大型心筋症，左室乳頭筋の肥大例，運動選手，QT短縮症候群などに認められると報告されており，J波の成因・機序に関しては，今後多方面からの詳細な検討が必要と考えられる．

C 原因遺伝子

これまで早期再分極症候群では，K_{ATP}電流（$I_{K,ATP}$）を増加させる*KCNJ8*遺伝子，L型Ca^{2+}電流（$I_{Ca,L}$）を低下させる*CACNA1C*, *CACNB2b*, *CACNAD1*遺伝子，Na^+電流を低下させる*SCN5A*遺伝子の変異が報告されている[5]．しかしながら，それらはいずれもBrugada症候群の原因遺伝子でもあり，報告された例の心電図をみると，T波陰転はないものの前胸部誘導はcoved型を呈していて，Brugada症候群と紛らわしいものが少なくない．

D 心電図陽性率，発症率

これまでに，1 mm以上のJ波は1回の心電図記録で数〜11%に認められるが，運動選手では陽性率が25〜44%に上昇すると報告されている．男性

には女性の2〜3倍多く存在し，その他に若年者，黒人，徐脈，左室肥大例で出現頻度が高くなる．運動選手には側壁の早期再分極が多いが，成人全体でみると下壁の早期再分極のほうが側壁よりも多い．Haruta らは，長崎原爆の被爆者を46年間経過観察した結果，下側壁誘導のJ波の発症率は年間0.7%で，Brugada 症候群の約50倍に相当し，心電図陽性率は初回の10.9%から加齢，記録回数とともに上昇して最終的には23.9%に達すると報告している[6]．

一方，VF の既往のある例では，J波の頻度は約30%に上り，下壁，高位側壁，側壁誘導の順に頻度が低下すると報告されている．またVF既往の運動選手ではST上昇を伴わないJ波が健常人に比し有意に多いことも指摘されている．

病態と予後

Haïssaguerre らはVFを合併した下側壁早期再分極症候群の一連の報告の中で，VFは睡眠中に20%が起こり，その連結期は260〜400 msecと短く，起源の2/3は左室である．電気生理学的検査（EPS）でのVF誘発率は34%で，経過観察中27%が複数回VFを生じる．VF直前にはJ波が増高するが，β遮断薬でも増高する．一方，イソプロテレノールではJ波は減高し，ストーム出現例ではイソプロテレノールによりVFが消失する．また予防にキニジンが有効であると述べている[1,7]．これらの特徴はBrugada 症候群に似ているが，睡眠中のVF発生率，EPSでのVF誘発率などは頻度が少なく，VFの1/3だけが右室から生じる点もやや異なっている．

VFの既往のない早期再分極例の予後に関しては，フィンランドのTikkanen らが10,864人の成人を約30年間後ろ向きに経過観察している[8]．それによると，側壁誘導のJ波は予後に関係しないが，下壁にJ波のある例は心臓死，不整脈死が有意に多い．またJ波の大きい例の予後が悪く，下壁誘導に2 mmを超えるJ波を有する例では，30年間で心臓死が約35%，不整脈死が約25%に生じたと報告している．この他に彼らは，下壁誘導のJ波例のなかでもJ波に続くST部がascending/upslopingの例の予後はよいが，horizontal/descendingの例は有意に不整脈死が多いとも述べている．Tikkanen らは下壁誘導で2 mm以上のJ波を持つ無症候性早期再分極症候群の年間不整脈死率は約0.8%程度と報告しており，この結果から下側壁早期再分極症候群の予後は，日本人の無症候性Brugada 症候群の予後と同等かそれ以下と考えられる．

一方，Haruta らも下側壁に早期再分極を伴う被爆者の予後を調査しており，それによると早期再分極があると不測死が有意に多く（ハザード比：1.8），とくに下壁および側壁にJ波のある患者，J波にslurとnotchの両方がある患者に不測死が多いと報告している[5]．

治療

前述のように，下側壁早期再分極症候群の一部ではイソプロテレノール，キニジン，シロスタゾールなどBrugada 症候群の治療が有効と報告されている．またVF既往例では植込み除細動器（ICD）植込みが必要と思われる．一方，早期再分極症候群に関しては前向きの予後が不明であり，不良な予後の予測因子も不明である．後ろ向き調査の結果からは無症候例の予後は良好と思われるが，一般人におけるJ波の陽性例が多いことから，機序の解明を含めた本症候群の総合的な診断・治療指針の確立が急務と考えられる．

文　献

1) Haissaguerre M et al: Sudden cardiac arrest associated with early repolarization. N Engl J Med 358: 2016-2023, 2008
2) Aizawa Y et al: Idiopathic ventricular fibrillation and bradycardia-dependent intraventricular block. Am J Cardiol 126: 1473-1474, 1993
3) Antzelevitch C et al: J wave syndromes. Heart Rhythm 7: 549-558, 2010
4) Kawata H et al: Effect of sodium-channel blockade on early repolarization in inferior/lateral leads in patients with idiopathic ventricular fibrillation and Brugada syndrome. Heart Rhythm 9: 77-83, 2011
5) Watanabe H et al: Electrocardiographic characteristics and SCN5A mutations in idiopathic ventricular fibrillation associated with early repolarization. Circ Arrhythm Electrophysiol 4: 874-881, 2011
6) Haruta D et al: Incidence and prognostic value of early repolarization pattern in the 12-lead electrocardiogram.

Circulation 123: 2931–2937, 2011
7) Haïssaguerre M et al: Characteristics of recurrent ventricular fibrillation associated with inferolateral early repolarization role of drug therapy. J Am Coll Cardiol 53: 612–619, 2009
8) Tikkanen JT et al: Long-term outcome associated with early repolarization on electrocardiography. N Engl J Med 361: 2529–2537, 2009

3. J波症候群

3.1 はじめに

J波症候群、または早期再分極（early repolarization）症候群は、Haissaguerreらが2008年に、下側壁誘導における下側壁早期再分極症候群という概念をNew Engl J Med誌に発表して以来[1]、急速に注目を集めている突然死疾患である。本疾患は基礎心疾患を伴わない特発性心室細動（VF）の1種であるBrugada症候群に類似しているが、Brugada症候群がV1-V3誘導でのcoved型、またはsaddleback型という特異的なST上昇を示すのに対し、主としてII、III、aVF誘導またはI、aVL、V4-V6誘導での1mm以上の波高のJ波（notch or slur）とそれに続くST上昇を特徴とする。一方、従来からV4-V6誘導での早期再分極波形が若年男性に多く存在することも知られており、これらは予後が良好と報告されていた。現時点で、J波症候群はその有病率、発症率、後ろ向き予後が判明しつつある段階であるが、発症機序、遺伝的背景は解明途中であり、前向きの予後、予後予測因子は未解明である。本稿では、現時点で判明しているJ波症候群の病態について述べる。

3.2 心電図所見

Haissaguerreの定義では、下側壁の早期再分極症候群とは前述の如く、側壁（I、aVL V4-V6）、または下壁（II、III、aVF）誘導のうち、連続する2誘導以上で1mm以上の高さのJ波とST上昇が認められる症例をさす（図1）。Haissaguerreらは早期再分極症候群から典型的なBrugada症候群、すなわちType1（coved型）のBrugada症候群を除外しているが、Type2、Type3などsaddleback型のBrugada波形を有する症例は除外していない。このため、Haissaguerreらの早期再分極症候群には前壁の早期再分極を合併するものが一部含まれると考えた方がよい。

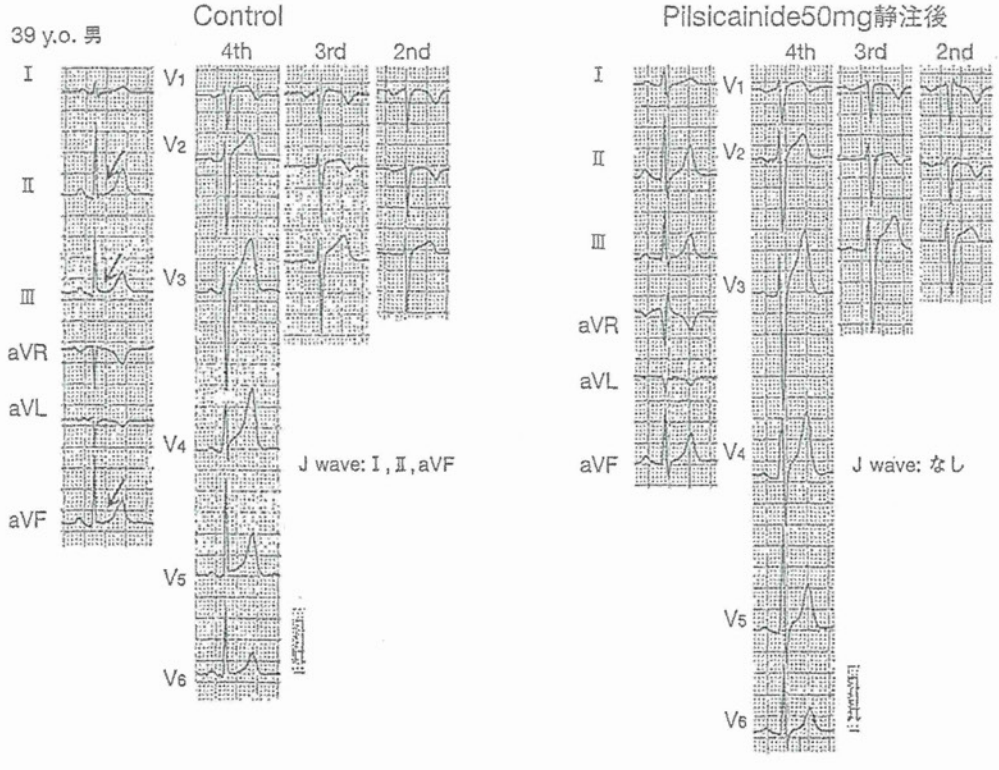

図1　J波症候群の12誘導心電図
39歳男性でVFの既往がある。ControlではII、III、aVF誘導にJ波(矢印)が認められるが、pilsicainide静注後は同誘導にS波が出現し、J波は消失している。

J波はBrugada波形と同様に、記録時期により形状や高さが異なる、または消失することもあるので、できるだけ多くの心電図で評価する必要がある。

3.3 J波と心室細動発生機序

J波の類似波形は低体温時に見られるOsborn波として知られているが、それ以前の1930年代から、J波は正常亜型の波形として健常成人の数%、特に若年男女に見られると報告されていた。一方、J波の存在する例でVFが生じることは1984年頃から報告されはじめ、AizawaやTakagiらが下壁誘導や側壁誘導でJ波の存在する複数例を報告している[2]。

このJ波とVFの機序に関しては、Antzelevitchらが動脈灌流心筋切片を用いたモデルで、心内膜側と心外膜側間に生じる貫壁性電位勾配の差で説明している。すなわち、活動電位第1相において、主として心室心外膜側に生じる一過性外向き電流（Ito）により、貫壁性電位勾配が生じてJ波が出現するが、遺伝子異常等により、内向きのNa電流やCa電流などが減少すると、Itoを含む相対的な外向き電流が増加して、活動電位第1相のnotchが大きくなり、心外膜－心内膜間に大きな電位勾配が生じる。それによりJ波の増大に引き続いてST上昇が起こる。さらに相対的な外向き電流が増加すると、心外膜側で第2相のdome形成が遅延または消失し、貫壁性および心外膜層内で再分極時間のばらつきが生じると共に、domeの消失した心筋において再脱分極がおこる。これはphase2 reentryと呼ばれ、これからVFが発生するとされている。

この理論はBrugada症候群におけるJ波とVFの発生機序でもあり、このためAntzelevitchらは早期再分極症候群とBrugada症候群が一連の疾患であるとして、それらをJ波症候群と総称して4つのタイプに分類している。すなわち側壁誘導にのみJ波が存在するものを早期再分極（ERS）Type1、下壁または下側壁誘導に存在するものをERS Type2、下壁と側壁、および前壁の広範囲誘導（global leads）に存在するものをERS Type3、そしてBrugada症候群とし、早期再分極症候群では1から3の順で危険性が増すとしている[3]。ただJ波が実際に、どの心電図誘導に出現するかは曖昧になっており、Type1ではⅠ、V4-V6誘導に、Type2ではⅡ、Ⅲ、aVF誘導に出現するとし、Type3はどの誘導で見られるかを示していない。

一方、J波が真に再分極の波形なのかを疑問視する報告もある。Surawiczらは、種々の論文で引用された早期再分極波形からJ波の時相を検討すると、J波はR波の一部にすぎない可能性があり、再分極の波形とは断言できないと述べている。またAbeらは加算平均心電図の検討から、J波は再分極異常よりも脱分極異常に由来するのではないかと述べている。Kawataらも下側壁誘導のJ波がNaチャネル遮断薬で減高することから、下側壁誘導のJ波はBrugada症候群に認められる前壁誘導のJ波とは機序が異なる可能性を指摘している[4]。

この他、J波は急性心筋虚血、肥大型心筋症、左室乳頭筋の肥大例、偽腱索例、運動選手、QT短縮症候群などに認められると報告されており、J波の成因・機序に関しては、今後多方面からの詳細な検討が必要と考えられる。

3.4 原因遺伝子

これまでJ波症候群では、K_{ATP}電流を増加させるKCNJ8遺伝子、L型Ca電流を低下させるCACNA1C、CACNB2b、CACNAD1遺伝子、Na電流を低下させるSCN5A遺伝子の変異が報告されている[5]。しかしながらそれらはいずれもBrugada症候群の原因遺伝子でもあり、報告された例の心電図を見ると、T波陰転はないものの前胸部誘導はcoved型を呈していて、Brugada症候群と紛らわしいものが少なくない。

3.5 心電図陽性率、発症率

これまでに、1 mm以上のJ波は、1回の心電図記録で数%から11%に認められるが、運動選手では陽性率が25%から44%に上昇すると報告されている。男性には女性の2～3倍多く存在し、その他に若年者、黒人、徐脈、左室肥大例で出現頻度が高くなる。運動選手には側壁の早期再分極が多いが、成人全体で見ると下壁の早期再分極の方が側壁よりも多い。Harutaらは、長崎原爆の被爆者を46年間経過観察した結果、下側壁誘導のJ波の発症率は年間0.7%で、Brugada症候群の約50倍に相当し、心電図陽性率は初回の10.9%から加齢、記録回数と共に上昇して最終的には23.9%に達すると報告している[6]。またJ波の疫学的特徴はBrugada症候群とは大きく異なると述べている。

一方、VFの既往のある例では、J波の頻度は約30%に上り、下壁、高位側壁、側壁誘導の順に頻度が低下すると報告されている。またVF既往の運動選手ではST上昇を伴わないJ波が健常人に比し有意に多いことも指摘されている。

3.6 病態と予後

Haissaguerre らは VF を合併した下側壁早期再分極症候群の一連の報告の中で、VF は睡眠中に 20％が起こり、その連結期は 260 ～ 400 msec と短く、起源の 2/3 は左室である。電気生理学検査（EPS）での VF 誘発率は 34％で、経過観察中 27％が複数回 VF を生じる。VF 直前には J 波が増高するが、β遮断薬でも増高する。一方、イソプロテレノールでは J 波は減高し、電気的ストーム出現例ではイソプロテレノールにより VF が消失する。また予防にキニジンが有効であると述べている[1,7]。これらの特徴は Brugada 症候群に似ているが、睡眠中の VF 発作率、EPS での VF 誘発率等は頻度が少なく、VF の 1/3 だけが右室から生じる点もやや異なっている。

VF の既往のない早期再分極例の予後に関しては、フィンランドの Tikkanen らが 10,864 人の成人を約 30 年間後ろ向きに経過観察している[8]。それによると、側壁誘導の J 波は予後に関係しないが、下壁に J 波のある例は心臓死、不整脈死が有意に多い。また J 波の大きい例の予後が悪く、下壁誘導に 2 mm を越える J 波を有する例では、30 年間で心臓死が約 35％、不整脈死が約 25％に生じたと報告している。この他に彼らは、下壁誘導の J 波例の中でも J 波に続く ST 部が ascending/upsloping の例の予後はよいが、horizontal/descending の例は有意に不整脈死が多いとも述べている。Tikkanen らは下壁誘導で 2 mm 以上の J 波をもつ無症候性早期再分極症候群の年間不整脈死率は約 0.8％程度と報告しており、この結果から下側壁早期再分極症候群の予後は、日本人の無症候性 Brugada 症候群の予後と同等かそれ以下と考えられる。

一方、Haruta らも下側壁に早期再分極を伴う被爆者の予後を調査しており、それによると早期再分極があると不測死が有意に多く（HR:1.8）、特に下壁および側壁に J 波のある人、J 波に slur と notch の両方がある人に不測死が多いと報告している[6]。

3.7 治療

前述の如く、下側壁早期再分極症候群または J 波症候群の一部ではイソプロテレノール、キニジン、シロスタゾールなど Brugada 症候群の治療が有効と報告されている。また VF 既往例では ICD 植込みが必要と思われる。一方、本症候群に関しては前向きの予後が不明であり、予後の予測因子も不明である。後ろ向き調査の結果からは無症候の J 波例の予後は良好と思われるが、一般人における J 波の陽性例が多いことから、機序の解明を含めた本症候群の総合的な診断・治療指針の確立が急務と考えられる。

3.8 おわりに

J 波症候群は再分極異常とみなす考えが主流であるが、病態からは脱分極異常所見も少なからず認められる。また J 波の定義やタイプ分類も確立されているとは言い難い。このため原因遺伝子や機序を含めて、J 波症候群の全貌が解明されるまでには今しばらくの時間を要すると思われる。

文献

1) Haïssaguerre M, et al: N Engl J Med 358: 2016-23, 2008
2) Aizawa Y, et al: Am J Cardiol 126: 1473-4, 1993
3) Antzelevitch C, et al: Heart Rhythm. 7: 549-558, 2010
4) Kawata H, et al: Heart Rhythm, 2011（in press）
5) Watanabe H, et al: Circ Arrhythm Electrophysiol 4: 874-881, 2011
6) Haruta D, et al: Circulation 123: 2931-7, 2011
7) Haïssaguerre M, et al: J Am Coll Cardiol 53: 612-9, 2009
8) Tikkanen JT, et al: N Engl J Med 361: 2529-37, 2009

（鎌倉史郎）

Prolyl Hydroxylase Domain Protein 2 Plays a Critical Role in Diet-Induced Obesity and Glucose Intolerance

Hirohide Matsuura, MD, PhD; Toshihiro Ichiki, MD, PhD; Eriko Inoue, MD; Masatoshi Nomura, MD, PhD; Ryohei Miyazaki, MD, PhD; Toru Hashimoto, MD, PhD; Jiro Ikeda, MD; Ryoichi Takayanagi, MD, PhD; Guo-Hua Fong, PhD; Kenji Sunagawa, MD, PhD

Background—Recent studies suggest that the oxygen-sensing pathway consisting of transcription factor hypoxia-inducible factor and prolyl hydroxylase domain proteins (PHDs) plays a critical role in glucose metabolism. However, the role of adipocyte PHD in the development of obesity has not been clarified. We examined whether deletion of *PHD2*, the main oxygen sensor, in adipocytes affects diet-induced obesity and associated metabolic abnormalities.

Methods and Results—To delete *PHD2* in adipocyte, *PHD2*-floxed mice were crossed with aP2-Cre transgenic mice (*Phd2$^{f/f}$/aP2-Cre*). *Phd2$^{f/f}$/aP2-Cre* mice were resistant to high-fat diet–induced obesity (36.7±1.7 versus 44.3±2.0 g in control; $P<0.01$) and showed better glucose tolerance and homeostasis model assessment–insulin resistance index than control mice (3.6±1.0 versus 11.1±2.1; $P<0.01$). The weight of white adipose tissue was lighter (epididymal fat, 758±35 versus 1208±507 mg in control; $P<0.01$) with a reduction in adipocyte size. Macrophage infiltration into white adipose tissue was also alleviated in *Phd2$^{f/f}$/aP2-Cre* mice. Target genes of hypoxia-inducible factor, including glycolytic enzymes and adiponectin, were upregulated in adipocytes of *Phd2$^{f/f}$/aP2-Cre* mice. Lipid content was decreased and uncoupling protein-1 expression was increased in brown adipose tissue of *Phd2$^{f/f}$/aP2-Cre* mice. Knockdown of PHD2 in 3T3L1 adipocytes induced a decrease in the glucose level and an increase in the lactate level in the supernatant with upregulation of glycolytic enzymes and reduced lipid accumulation.

Conclusions—PHD2 in adipose tissue plays a critical role in the development of diet-induced obesity and glucose intolerance. PHD2 might be a novel target molecule for the treatment of obesity and associated metabolic abnormalities. **(*Circulation*. 2013;127:2078–2087.)**

Key Words: adipocytes ■ cell hypoxia ■ obesity ■ prolyl hydroxylase domain protein

Obesity is one of the critical risk factors for the development of atherosclerosis, diabetes mellitus, and coronary artery disease.[1] Previous studies have shown that obesity induces low-grade chronic inflammation in adipose tissue,[2] leading to dysregulated adipocytokine production and increased oxidative stress.[3–5] These contribute to the pathogenesis of glucose intolerance, dyslipidemia, and insulin resistance in obesity. To prevent these adverse effects in obese patients, body weight reduction is necessary. Although patient education on lifestyle modification and the encouragement of physical exercise are recommended to normalize body weight, the effects are often insufficient. Therefore, alternative means to ameliorate obesity have been attempted such as the development of antiobesity drugs.[6] The cannabinoid-1 receptor blocker rimonabant was developed with great expectation,[7] but it has not been commonly used in clinical practice because of side effects such as depression and anxiety disorder.[8] Thus, a novel therapeutic target to treat obesity is sought.

Clinical Perspective on p 2087

Hypoxia has long been known to reduce body weight in both humans[9] and animals.[10,11] Although hypoxia is shown to suppress fatty acid synthesis and to reduce fat mass,[12,13] the mechanism has not been clarified. Recently, the role of the oxygen-sensing pathway in metabolism has received much attention. The oxygen-sensing pathway consists of a transcription factor, hypoxia-inducible factor (HIF), that is a heterodimer of HIF-α and HIF-β and an oxygen sensor, prolyl hydroxylase domain protein (PHD).[14] PHD catalyzes oxygen-dependent hydroxylation of the specific proline residues in HIF-α subunits, a modification that tags HIF-α for rapid polyubiquitination and subsequent proteasomal degradation. Hypoxia increases HIF expression by diminishing PHD activities, thereby activating the expression of divergent target genes involved in metabolism and angiogenesis.

Received April 8, 2012; accepted April 18, 2013.

From the Departments of Cardiovascular Medicine (H.M., T.I., E.I., R.M., T.H., J.I., K.S.), Advanced Therapeutics for Cardiovascular Diseases (T.I.), and Medicine and Bioregulatory Science (M.N., R.T.), Kyushu University Graduate School of Medical Sciences, Fukuoka, Japan; and Center for Vascular Biology, Department of Cell Biology, University of Connecticut Health Center, Farmington (G.-H.F.).

The online-only Data Supplement is available with this article at http://circ.ahajournals.org/lookup/suppl/doi:10.1161/CIRCULATIONAHA.113.001742/-/DC1.

Correspondence to Toshihiro Ichiki, MD, PhD, Department of Advanced Therapeutics for Cardiovascular Diseases, Kyushu University Graduate School of Medical Sciences, Fukuoka, Japan. E-mail ichiki@cardiol.med.kyushu-u.ac.jp

Circulation **is available at http://circ.ahajournals.org** **DOI: 10.1161/CIRCULATIONAHA.113.001742**

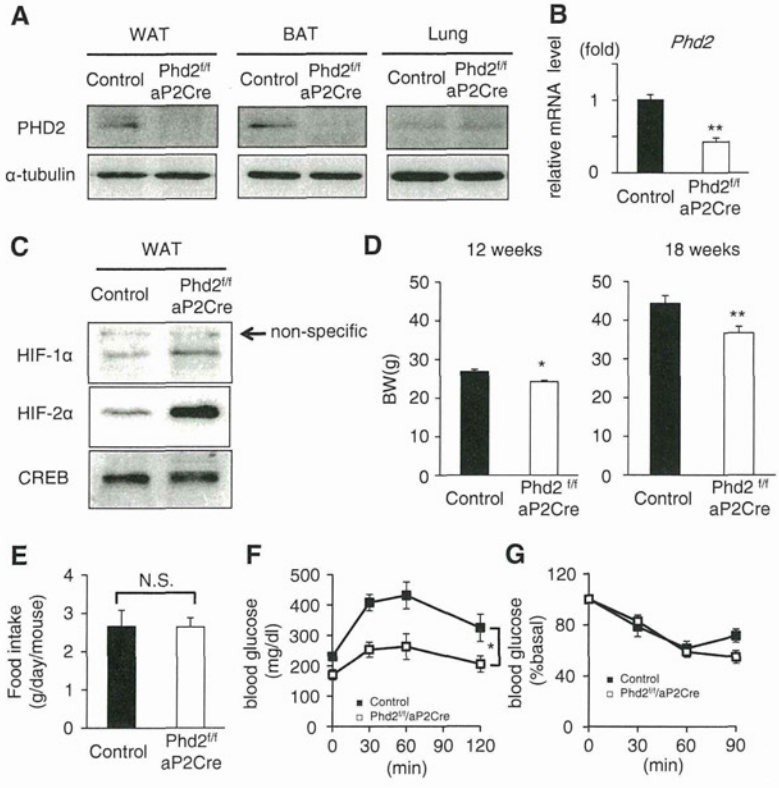

Figure 1. *Phd2f/f/aP2-Cre* mice were resistant to diet-induced obesity with better glucose tolerance. **A,** Western blot analysis for prolyl hydroxylase domain protein 2 (PHD2) in epididymal white adipose tissue (WAT), brown adipose tissue (BAT), and lung in control and *Phd2f/f/aP2-Cre* mice is shown. As a loading control, Western blotting for α-tubulin was performed. The same results were obtained in other independent experiments. n=3. **B,** The result of real-time quantitative polymerase chain reaction analysis of WAT for *Phd2* in control and *Phd2f/f/aP2-Cre* mice is shown in the bar graph. n=6. ***P*<0.01 vs control. **C,** Western blot analysis for hypoxia-inducible factor (HIF)-1α, HIF-2α, and cAMP response element binding protein (CREB) using nuclear extracts from WAT is shown. Bar graphs in Figure IE in the online-only Data Supplement indicate statistical analysis. n=3. **P*<0.05. **D,** Twelve-week-old control or *Phd2f/f/aP2-Cre* mice were fed a high-fat diet (HFD) for 6 weeks. Body weight (BW) at 12 and 18 weeks is shown in the bar graphs. n=6 to 7. **P*<0.05, ***P*<0.01 vs control. **E,** The amount of food intake in both groups fed an HFD is shown in the bar graph. n=6 to 7. **F,** Control (black box) and *Phd2f/f/aP2-Cre* (white box) mice fed an HFD for 6 weeks were injected intraperitoneally with glucose, and blood glucose levels were measured. n=6 to 7. **P*<0.05 vs control. **G,** Control (black box) and *Phd2f/f/aP2-Cre* (white box) mice fed an HFD for 6 weeks were injected intraperitoneally with insulin, and blood glucose levels were measured. n=6 to 7.

Several cell culture studies have revealed that hypoxia and HIF convert cell metabolism that is dependent on aerobic glucose oxidation and fatty acid synthesis into that which is dependent on anaerobic glycolysis. HIF not only upregulates a series of glycolytic enzymes[15,16] but also actively inhibits oxidative phosphorylation in mitochondria by inducing pyruvate dehydrogenase kinase 1 (PDK1).[17,18] PDK1 inhibits pyruvate dehydrogenase activity and consequently reduces the conversion of pyruvate to acetyl CoA, an essential substrate for oxidative phosphorylation.[17,18] In addition, HIF inhibits adipogenesis by inducing DEC1/Stra13.[13] These HIF-induced metabolic alterations such as increased glucose consumption and less fatty acid synthesis might be beneficial for nutrient excess in obese or diabetic subjects. Although HIF could be a potential therapeutic target, direct manipulation of HIF is often difficult in vivo. In contrast, PHD is an ideal target to manipulate HIF levels, and several chemical inhibitors of PHD have been developed.[19] However, the role of adipocyte PHD in the development of obesity-induced glucose intolerance has not been determined. In the present study, we generated mice lacking PHD2, also known as Egl 9 homolog1 (EglN1) in adipocytes, because PHD2 is the most crucial isoform to regulate HIF level in vitro[20] and in vivo[21] among 3 PHD isoforms (PHD1, PHD2, and PHD3). We found that *PHD2* deletion in adipocyte attenuates weight gain and alleviates glucose intolerance induced by a high-fat diet (HFD).

Methods

Additional details of the experimental procedures are included in the online-only Data Supplement.

All animal procedures were approved by the Animal Care and Use Committee of Kyushu University and conducted in accordance with the institutional guidelines. Previously generated *Phd2*-floxed mice (*Phd2f/+*)[21] were crossed with transgenic mice expressing Cre recombinase under control of the *aP2* gene promoter (*aP2-Cre*), resulting in the generation of *Phd2f/+/aP2-Cre* mice. Then, *Phd2f/f/aP2-Cre* mice were generated by stepwise crossing of *Phd2f/+/aP2-Cre* mice with *Phd2f/f* mice. *Phd2f/f* mice served as controls. These mice were fed an HFD containing 60% kcal fat (High Fat Diet 32, Clea Japan, Inc) from 12 to 18 weeks of age. Mice 12 and 18 weeks of age were analyzed. Preparation of cell lysate and total RNA, Western blot analysis, quantitative reverse transcription–polymerase chain reaction, luciferase assay, and histological/immunohistochemical analysis were performed using conventional methods. The primer sequences for quantitative reverse transcription–polymerase chain reaction are shown in Table I in the online-only Data Supplement. Serum concentrations of glucose, cholesterol, triglyceride, insulin, lactate, and cytokines were determined by commercially available kits. Oxygen consumption was measured with a computer-controlled open-circuit indirect calorimeter. Normality and homoscedasticity of the data were assessed by the Shapiro-Wilk test and Levene test, respectively. A *t* test or exact binomial test was used for pairwise comparisons. Multiple comparisons were performed with 1-way or 2-way ANOVA. The Fisher post hoc test was used if appropriate. Data are shown as mean±SEM. Values of $P<0.05$ were considered significant. Detailed methods are given in the online-only Data Supplement.

Results

PHD2-Deficient Mice Showed Better Glucose Tolerance After HFD Feeding

PHD2 protein was reduced in white adipose tissue (WAT) and brown adipose tissue (BAT) but not in other organs such as lung and skeletal muscle in PHD2-deficient mice (*Phd2f/f/aP2-Cre*; Figure 1A and Figure IA in the online-only Data Supplement). Expression of PHD2 in heart and bone marrow–derived macrophages was slightly reduced. We did not find any apparent abnormalities in the appearance in *Phd2f/f/aP2-Cre* mice. *Phd2* mRNA was significantly decreased in WAT from *Phd2f/f/aP2-Cre* mice (Figure 1B). We then separated

Table. Serum Chemistry of Control and *Phd2$^{f/f}$/aP2-Cre* Mice

Parameters	Control (n=6)	*Phd2$^{f/f}$/aP2-Cre* (n=6)	*P* Values
Fasting glucose, mg/dL			
Normal chow	138±7	122±9	0.23
HFD	230±11	158±16	<0.01
Fasting insulin, ng/mL			
Normal chow	0.71±0.10	0.65±0.12	0.74
HFD	2.10±0.34	0.79±0.17	<0.01
HOMA-IR			
Normal chow	4.07±0.58	3.68±0.78	0.23
HFD	11.10±2.14	3.60±0.99	<0.01
Total cholesterol, HFD, mg/dL	163±11	171±16	0.69
Triglycerides, HFD, mg/dL	84±3	89±3	0.28
Lactate, nmol/μL			
Normal chow	6.4±0.5	5.6±0.5	0.34
HFD	11.3±0.5	8.5±1.0	<0.05

HFD indicates high-fat diet; and HOMA-IR; homeostasis model assessment–insulin resistance: (fasting glucose×fasting insulin)/22.5.

an adipocyte-rich fraction and a stromal vascular fraction of WAT (Figure IB in the online-only Data Supplement) and examined the expression of *Phd2* mRNA. Expression of *Phd2* mRNA was significantly reduced in the adipocyte-rich fraction of WAT (Figure IC in the online-only Data Supplement). Expression of *Phd2* mRNA was modestly reduced in the stromal vascular fraction, but the difference was not significant. The *Phd1* mRNA level was not changed and the *Phd3* mRNA level was increased several-fold in WAT of *Phd2$^{f/f}$/aP2-Cre* mice (Figure ID in the online-only Data Supplement). Both HIF-1α and HIF-2α proteins were significantly increased in PHD2-deficient WAT (Figure 1C and Figure IE in the online-only Data Supplement), confirming that PHD1 and PHD3 cannot compensate for the absence of PHD2 in terms of HIF-α degradation.

Body weight in *Phd2$^{f/f}$/aP2-Cre* mice was slightly lighter than in control mice (Figure 1D). After 6 weeks of HFD, *Phd2$^{f/f}$/aP2-Cre* mice gained significantly less body weight than controls. Food intake was comparable between the 2 groups (Figure 1E), and we did not find any abnormalities in the feces. These data suggest that *Phd2$^{f/f}$/aP2-Cre* mice were resistant to HFD-induced obesity.

Before HFD, glucose tolerance was comparable between controls and *Phd2$^{f/f}$/aP2-Cre* mice (Figure IIA in the online-only Data Supplement). After 6 weeks of HFD, control mice developed severe glucose intolerance, whereas *Phd2$^{f/f}$/aP2-Cre* mice showed significantly better glucose tolerance (Figure 1F). Although an insulin tolerance test revealed significantly lower glucose levels at all time points in *Phd2$^{f/f}$/aP2-Cre* mice on an HFD (Figure IIB in the online-only Data Supplement), the relative decrease in the glucose level from baseline was not different between control and *Phd2$^{f/f}$/aP2-Cre* mice (Figure 1G). *Phd2$^{f/f}$/aP2-Cre* mice showed lower fasting glucose level with a lower insulin concentration and hence a lower homeostasis model assessment–insulin resistance score (Table), suggesting that insulin sensitivity may also be improved in *Phd2$^{f/f}$/aP2-Cre* mice. Serum cholesterol and triglyceride levels were not different between control and *Phd2$^{f/f}$/aP2-Cre* mice (Table).

WAT Was Lighter in Weight and Adipocytes Were Smaller in *Phd2$^{f/f}$/aP2-Cre* Mice

After 6 weeks of HFD, the epididymal WAT of *Phd2$^{f/f}$/aP2-Cre* mice was smaller in size and significantly lighter in weight than that of controls (Figure 2A and Table II in the online-only Data Supplement). The perirenal WAT was also significantly lighter in weight in *Phd2$^{f/f}$/aP2-Cre* mice (Table II in the online-only Data Supplement). Liver weight was slightly smaller in *Phd2$^{f/f}$/aP2-Cre* mice, but the difference was not statistically significant. The weight of other organs such as heart, spleen, and kidney was not significantly different between the 2 groups. Histological analysis of epididymal WAT revealed that the size of adipocytes in *Phd2$^{f/f}$/aP2-Cre* mice was almost the same as that in control mice before HFD (Figure 2B and 2D). However, the extent of HFD-induced adipocyte hypertrophy was significantly reduced in *Phd2$^{f/f}$/aP2-Cre* mice compared with control mice (Figure 2C and 2D). A detailed analysis of the size distribution of the adipocytes revealed that WAT from controls contained a greater number of larger adipocytes (>10000 μm^2) than that

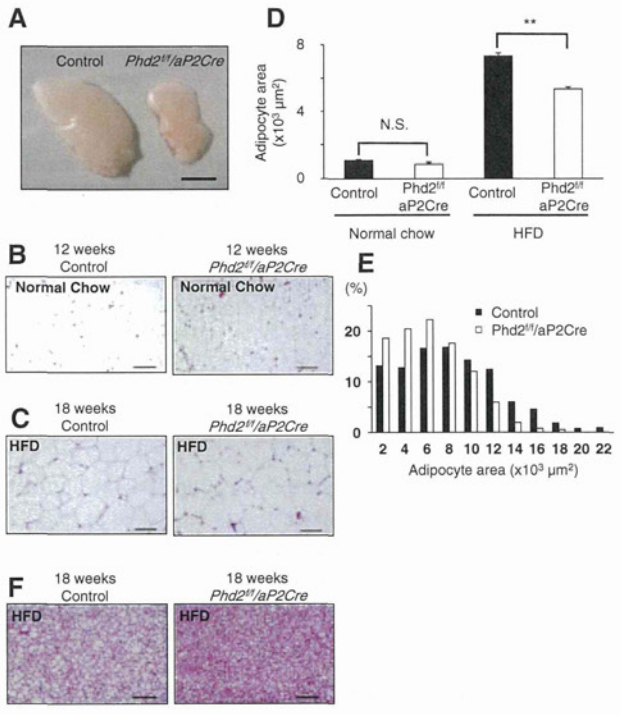

Figure 2. *Phd2$^{f/f}$/aP2-Cre* mice showed reduced fat mass. **A,** Representative pictures of epididymal white adipose tissue (WAT) from control and *Phd2$^{f/f}$/aP2-Cre* mice fed a high-fat diet (HFD) for 6 weeks are shown. Scale bar, 10 mm. **B** and **C,** Representative pictures of hematoxylin and eosin–stained sections of epididymal WAT from control and *Phd2$^{f/f}$/aP2-Cre* mice at 12 weeks (**B**) and after 6 weeks of an HFD (**C**) are shown. Scale bar=100 μm. **D,** The average cross-sectional area of adipocytes in epididymal WAT is shown in the bar graph. n=6 to 7. ***P*<0.01. **E,** The distribution of adipocyte cross-sectional area in epididymal WAT of HFD-fed control (black bar) or *Phd2$^{f/f}$/aP2-Cre* (white bar) mice is shown in the bar graph. n=6 to 7. **F,** Representative pictures of hematoxylin and eosin–stained sections of brown adipose tissue from HFD-fed control and *Phd2$^{f/f}$/aP2-Cre* mice are shown. Scale bar, 100 μm.

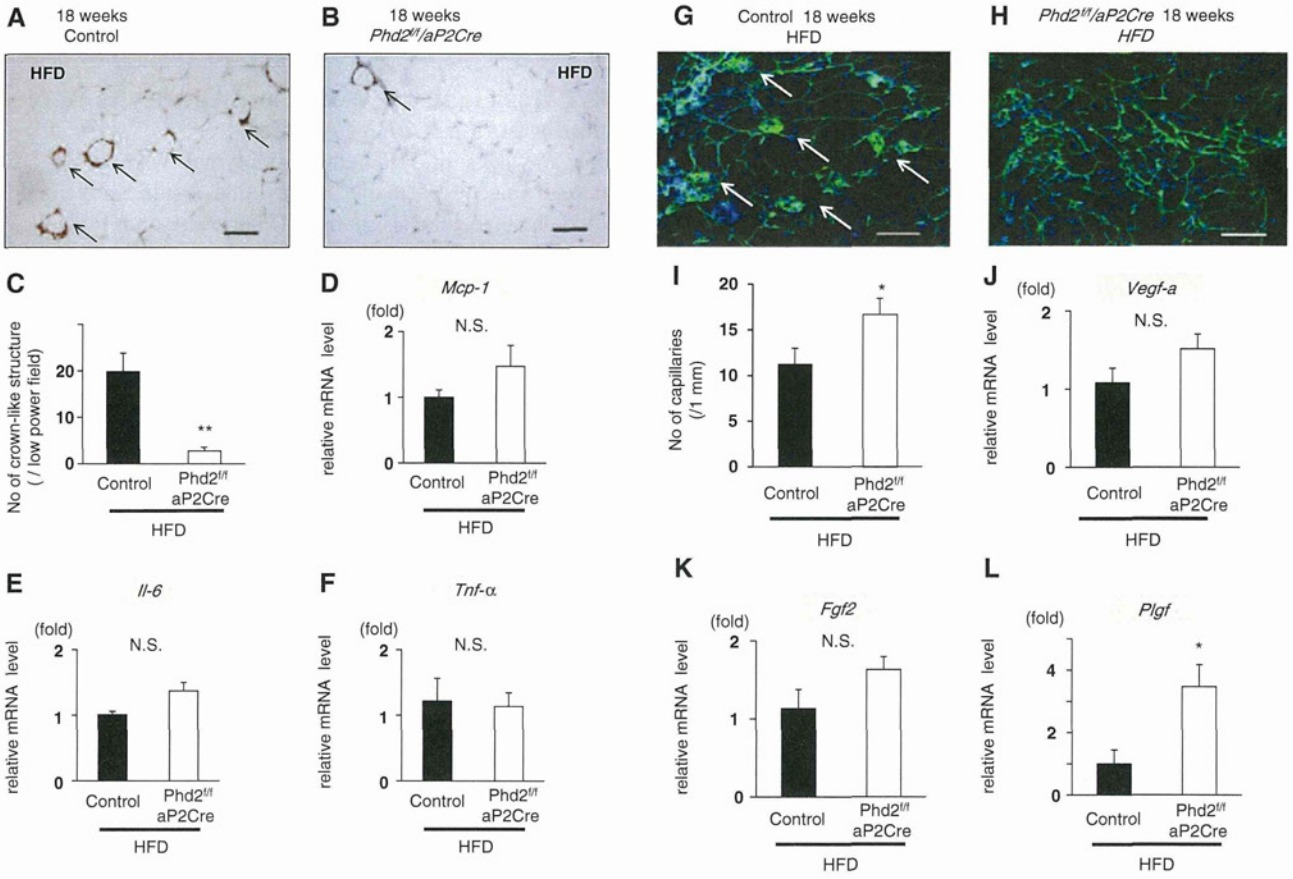

Figure 3. White adipose tissue (WAT) of *Phd2f/f/aP2-Cre* mice showed reduced macrophage infiltration and increased angiogenesis. **A** and **B**, Representative pictures of anti-Mac3 immunohistochemical analysis of macrophage aggregation in WAT of high-fat diet (HFD)–fed control (**A**) and *Phd2f/f/aP2-Cre* (**B**) mice are shown. Macrophage aggregation surrounding adipocytes (crown-like structure) is indicated by arrows. **C,** The number of crown-like structures is shown in the bar graph. n=5 to 6. $^{**}P<0.01$ vs control. Exact binomial test was used. **D** through **F,** The results of real-time quantitative polymerase chain reaction (qPCR) analysis for monocyte chemoattractant protein-1 (*Mcp-1*), interleukin-6 (*Il-6*), and tumor necrosis factor-α (*Tnf-α*) of WAT from HFD-fed control and *Phd2f/f/aP2-Cre* mice are shown in the bar graphs. n=6. **G** and **H**, Representative pictures of epididymal WAT from HFD-fed control and *Phd2f/f/aP2-Cre* mice stained with endothelial cell–specific lectin (green) are shown. Nuclei were counterstained with DAPI (blue). Scale bar, 100 μm. **I,** Quantification of vascular density in **G** and **H** is shown in the bar graphs. n=4 to 5. $^{*}P<0.05$ vs control. Exact binomial test was used. **J** through **L**, The results of real-time qPCR analyses for vascular endothelial growth factor-a (*Vegf-a*; **J**), fibroblast growth factor 2 (*Fgf2*; **K**), and placental growth factor (*Plgf;* **L**) are shown in the bar graphs. n=6. $^{*}P<0.05$ vs control. N.S. indicates not significant.

from *Phd2f/f/aP2-Cre* mice (Figure 2E). In contrast, the number of smaller adipocytes (< 10 000 μm^2) was increased in *Phd2f/f/aP2-Cre* mice compared with control mice (Figure 2E).

Lipid particles of adipocytes in BAT from HFD-fed *Phd2f/f/aP2-Cre* mice were apparently smaller compared with those from controls (Figure 2F).

Macrophage Infiltration Was Reduced in WAT of HFD-Fed *Phd2f/f/aP2-Cre* Mice

Chronic inflammation is reported as a common feature in the adipose tissue of obese subjects.[2,22] The macrophage aggregation surrounding adipocytes, often referred to as a crown-like structure,[23,24] was significantly decreased in WAT from HFD-fed *Phd2f/f/aP2-Cre* mice compared with controls (Figure 3A–3C). However, the expression of proinflammatory cytokines, including monocyte chemoattractant protein-1 (*Mcp-1*), interleukin-6 (*Il-6*), and tumor necrosis factor-α (*Tnf-α*), in WAT (Figure 3D–3F) and BAT (data not shown) was not significantly different between HFD-fed controls and *Phd2f/f/aP2-Cre* mice.

Serum levels of these cytokines were comparable between control and *Phd2f/f/aP2-Cre* mice (Figure III in the online-only Data Supplement).

Enhanced Angiogenesis in WAT From HFD-Fed *Phd2f/f/aP2-Cre* Mice

Because abnormal angiogenesis in WAT is reported as a common feature in obesity,[2,22] we examined the state of angiogenesis in HFD-fed controls and *Phd2f/f/aP2-Cre* mice. Endothelial cell–specific lectin staining demonstrated that vascular density was mildly increased in WAT from *Phd2f/f/aP2-Cre* mice compared with controls (Figure 3G–3I). We also determined the expression of several angiogenic factors such as vascular endothelial growth factor-a (*Vegf-a*), fibroblast growth factor 2 (*Fgf2*), and placental growth factor (*Plgf*) in WAT. Although the expression of *Vegf*-a and *Fgf2* remained almost the same between controls and *Phd2f/f/aP2-Cre* mice fed an HFD, the expression of *Plgf* was increased in HFD-fed *Phd2f/f/aP2-Cre* mice (Figures 3J–3L).

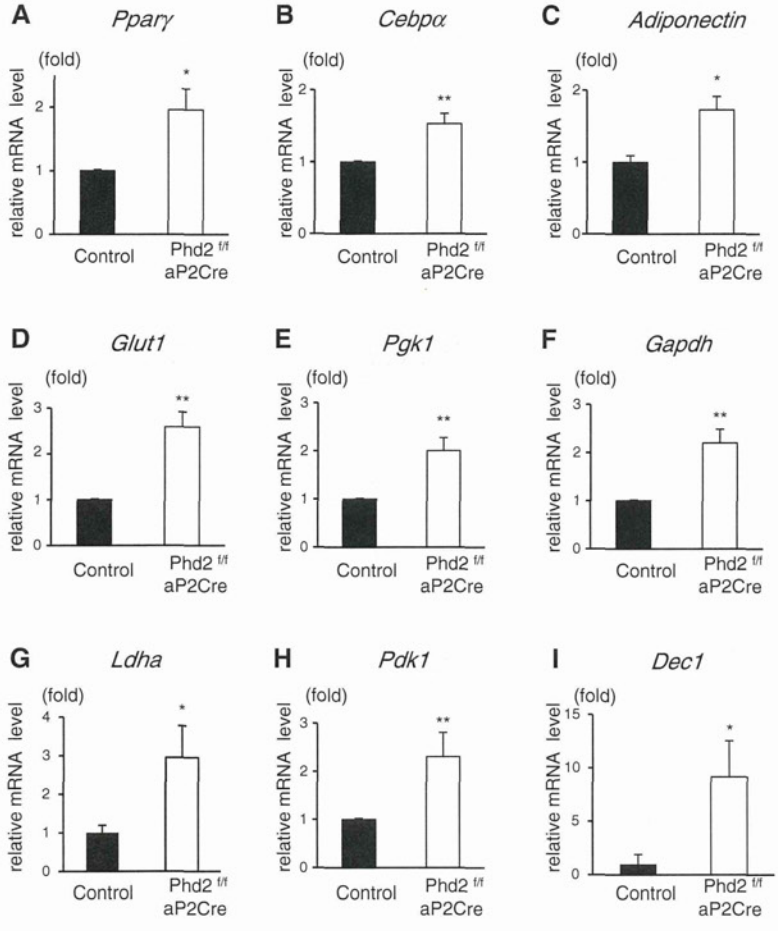

Figure 4. Expression of adipocyte differentiation markers and glycolytic enzymes was increased in the adipocyte-rich fraction from *Phd2$^{f/f}$/aP2-Cre* mice. Total RNA was extracted from the adipocyte-rich fraction of high-fat diet–fed control and *Phd2$^{f/f}$/aP2-Cre* mice. The results of real-time quantitative polymerase chain reaction analyses for (**A**) peroxisome proliferator activated receptor-γ (*Pparγ*), (**B**) CCAAT/enhancer binding protein α (*Cebpα*), (**C**) adiponectin, (**D**) glucose transporter 1 (*Glut1*), (**E**) phosphoglycerate kinase 1 (*Pgk1*), (**F**) glyceraldehyde-3-phosphate dehydrogenase (*Gapdh*), (**G**) lactate dehydrogenasea (*Ldha*), (**H**) pyruvate dehydrogenase kinase 1 (*Pdk1*), and (**I**) DEC-1/Stra13 are shown in the bar graphs. n=6. *P<0.05, **P<0.01 vs control.

Adipocyte Differentiation Markers and Glycolytic Enzymes Were Increased in Isolated Adipocytes of WAT in HFD-Fed *Phd2$^{f/f}$/aP2-Cre* Mice

We determined the expression of adipogenic markers in an adipocyte-rich fraction isolated from WAT of *Phd2$^{f/f}$/aP2-Cre* mice and controls to exclude the effect of stromal vascular cells. The expression of peroxisome proliferator-activated receptor-γ (*Pparγ*), CCAAT/enhancer binding protein α (*Cebp* α), and adiponectin was increased in the adipocyte-rich fraction of HFD-fed *Phd2$^{f/f}$/aP2-Cre* mice (Figure 4A–4C). However, the serum adiponectin concentration was not significantly different between control and *Phd2$^{f/f}$/aP2-Cre* mice (Figure III in the online-only Data Supplement).

Expression of Glucose Transporter and Glycolytic Enzymes Was Upregulated in Isolated Adipocytes From WAT of HFD-Fed *Phd2$^{f/f}$/aP2-Cre* Mice

Because HIF is known to activate glycolytic pathway,[17] we analyzed the expression of genes involved in glycolysis. The expression of glucose transporter 1 (*Glut1*) and several glycolytic enzymes such as phosphoglycerate kinase (*Pgk1*), glyceraldehyde-3-phosphate dehydrogenase (*Gapdh*), and lactate dehydrogenase-a (*Ldha*) was significantly upregulated in the adipocyte-rich fraction isolated from WAT of *Phd2$^{f/f}$/aP2-Cre* mice (Figure 4D–4G). In addition, the expression of pyruvate dehydrogenase kinase 1 (*Pdk1*), a rate-limiting enzyme of oxidative phosphorylation, was also significantly upregulated (Figure 4H). *Dec1*, which inhibits adipogenesis,[13] was also upregulated in *Phd2$^{f/f}$/aP2-Cre* mice (Figure 4I).

Unexpectedly, however, the serum lactate level was rather decreased in HFD-fed *Phd2$^{f/f}$/aP2-Cre* mice despite the upregulated expression of glycolytic enzymes (Table). We examined LDHa protein expression and found that LDHa protein was actually increased in WAT of *Phd2$^{f/f}$/aP2-Cre* mice (Figure IVA in the online-only Data Supplement).

Phd2$^{f/f}$/aP2-Cre Mice Showed Increased Oxygen Consumption With Uncoupling Protein-1 Upregulation

Oxygen consumption (Vo_2) was significantly increased in HFD-fed *Phd2$^{f/f}$/aP2-Cre* mice in both the light and dark periods (Figure 5A). Carbon dioxide production (Vco_2) was slightly increased in *Phd2$^{f/f}$/aP2-Cre* mice, but the difference was not statistically significant (Figure 5B). The respiratory exchange ratio was significantly lower in *Phd2$^{f/f}$/aP2-Cre* mice during the dark period when mice were active, but there was no difference during the light period (Figure 5C). The expression of *Ucp1*, one of the critical genes controlling the energy expenditure, was significantly upregulated in HFD-fed PHD2-deficient BAT compared with controls (Figure 5D). These data suggest that *PHD2* deletion in adipocytes increased energy expenditure using lipid at least partly mediated by upregulation of *Ucp1* in BAT.

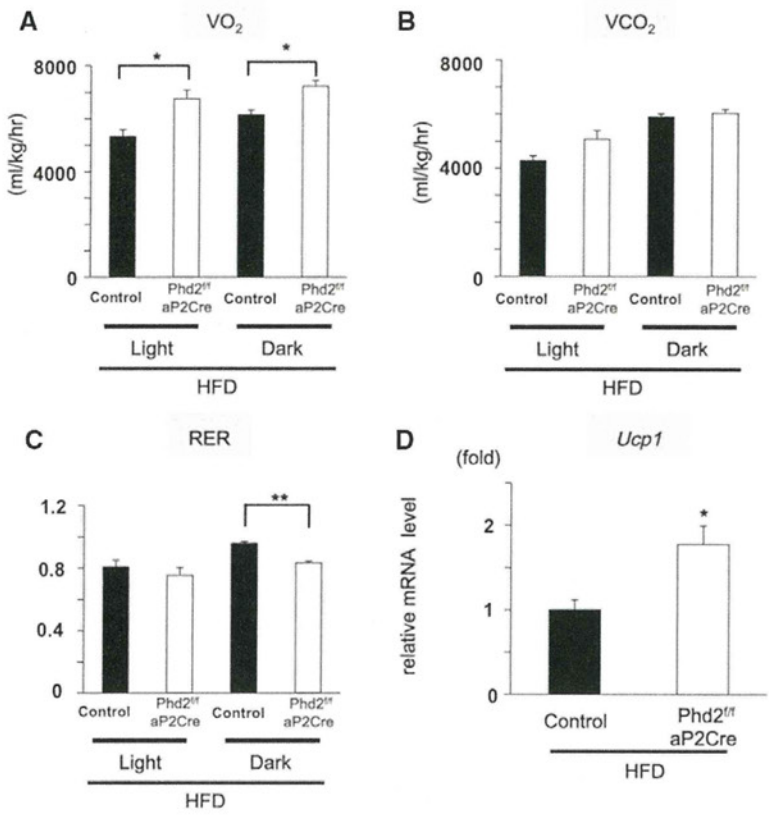

Figure 5. Oxygen consumption was increased in *Phd2$^{f/f}$/aP2-Cre* mice. **A** through **C,** High-fat diet (HFD)–fed control and *Phd2$^{f/f}$/aP2-Cre* mice were housed in a computer-controlled open-circuit indirect calorimeter to determine (**A**) oxygen consumption, (**B**) carbon dioxide production, and (**C**) respiratory exchange ratio (RER) during the light (8 am–8 pm) and dark (8 pm–8 am) periods. n=3. *P<0.05, **P<0.01. **D,** The result of real-time quantitative polymerase chain reaction analysis for uncoupling protein-1 (*Ucp*-1) in brown adipose tissue from HFD-fed control and *Phd2$^{f/f}$/aP2-Cre* mice is shown in the bar graph. n=6, *P<0.05 vs control.

Glut4 in Skeletal Muscle in *Phd2$^{f/f}$/aP2-Cre* Mice Was Upregulated

The expression of *Glut4* in skeletal muscle (quadriceps femoris muscle) of *Phd2$^{f/f}$/aP2-Cre* mice was significantly upregulated compared with controls (Figure 6A). Because Glut4 is downstream of insulin signaling, we examined the insulin signaling pathway in skeletal muscle. Expression of Glut4 protein and phosphorylation of Akt were increased in *Phd2$^{f/f}$/aP2-Cre* mice, which may support the idea that insulin sensitivity is improved in *Phd2$^{f/f}$/aP2-Cre* mice (Figure IVB in the online-only Data Supplement). The expression of genes involved in fatty acid oxidation such as acyl-CoA oxidase, carnitine palmitoyltransferase-1, and medium-chain acyl-CoA dehydrogenase in skeletal muscle was comparable between controls and *Phd2$^{f/f}$/aP2-Cre* mice, suggesting that fatty acid oxidation was not increased in skeletal muscle of *Phd2$^{f/f}$/aP2-Cre* mice (Figure 6B–6D). The expression of genes involved in hepatic gluconeogenic enzymes such as phosphoenolpyruvate carboxykinase and glucose-6-phosphatase was not different between the 2 mouse groups, suggesting that gluconeogenesis in the liver is not affected by *PHD2* deletion in the adipocytes (Figure 6E and 6F).

Glycolysis Was Promoted and Lipid Accumulation Was Suppressed in PHD2-Deficient 3T3-L1 Cells

To confirm that PHD2 deficiency increases glycolysis and attenuates lipid accumulation in adipocytes, we specifically knocked down *Phd2* mRNA by *Phd2*-specific shRNA in 3T3-L1 cells. The expression of both *Phd2* mRNA and PHD2 protein was significantly decreased in PHD2-deficient 3T3-L1 preadipocytes (Figure 7A and 7B). Hypoxia responsive element–dependent luciferase activity was significantly increased (Figure 7C).

In agreement with the results of in vivo experiments, the expression of *Glut1*, *Pgk1*, *Gapdh*, *Ldha*, and *Pdk1* was significantly upregulated in PHD2-deficient 3T3-L1 preadipocytes (Figure 7D). After the induction of adipocyte differentiation, the expression of Glut1 was reduced in PHD2-deficient 3T3-L1 adipocytes, whereas the expression of other genes was still significantly upregulated (Figure 7E). Both glucose consumption and lactate production in the supernatant were significantly increased in PHD2-deficient 3T3-L1 preadipocytes compared with control 3T3-L1 preadipocytes (Figure 7F and 7G), indicating acceleration of glycolysis. We also assessed de novo lipogenesis because PDK1 suppresses acetyl-CoA production, which is essential for fatty acid synthesis.[25] Oil Red O staining revealed that PHD2-deficient 3T3-L1 cells accumulated less lipid than control 3T3L-1 cells (Figure 7H and 7I).

Discussion

In this study, we demonstrated that *PHD2* deletion in adipocyte alleviates diet-induced obesity and glucose intolerance in mice. *PHD2* deletion reduced fat mass and macrophage infiltration into WAT and increased the expression of UCP-1 in BAT and oxygen consumption, all of which are supposed to be responsible for body weight reduction and better glucose tolerance in HFD-fed *Phd2$^{f/f}$/aP2-Cre* mice. The improvement in the glucose tolerance test was remarkable compared with the improvement in the insulin tolerance test under HFD, indicating that an improvement of insulin sensitivity may not be the

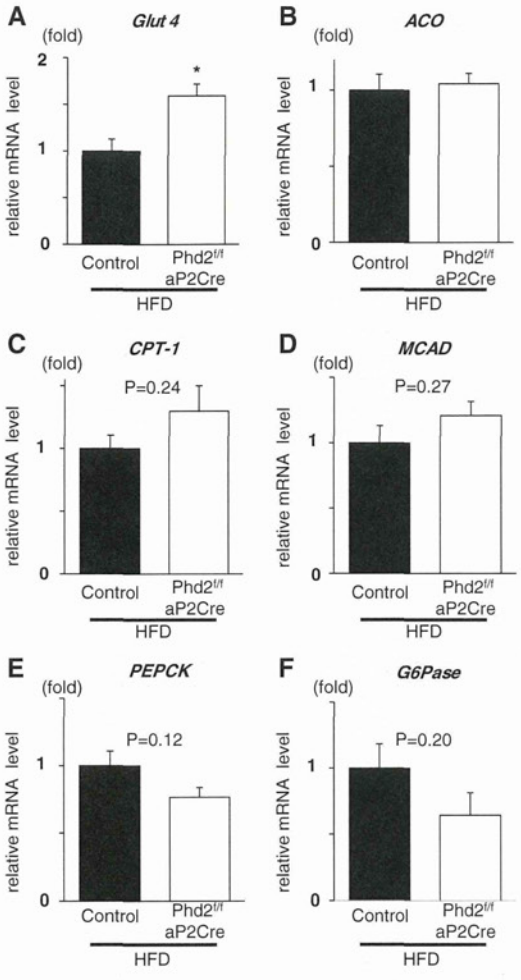

Figure 6. Glucose transporter 4 (Glut4) in skeletal muscle in *Phd2$^{f/f}$/aP2-Cre* mice was upregulated. **A** through **D**, Total RNA was extracted from skeletal muscle (quadriceps femoris muscle) of high-fat diet (HFD)–fed control and *Phd2$^{f/f}$/aP2-Cre* mice. The results of real-time quantitative polymerase chain reaction (qPCR) analyses for (**A**) *Glut4,* (**B**) acyl-CoA oxidase (*ACO*), (**C**) carnitine palmitoyltransferase-1 (*CPT-1*), and (**D**) medium-chain acyl-CoA dehydrogenase (*MCAD*) are shown in the bar graphs. n=6. *P<0.05 vs control. **E** and **F**, Total RNA was extracted from liver of HFD-fed control and *Phd2$^{f/f}$/aP2-Cre* mice. The results of real-time qPCR analyses for (**E**) phosphoenolpyruvate carboxykinase (*PEPCK*) and (**F**) glucose-6-phosphatase (*G6Pase*) are shown in the bar graphs. n=6.

primary effect of PHD2 deficiency. However, improvement in the homeostasis model assessment–insulin resistance suggests that insulin sensitivity in *Phd2$^{f/f}$/aP2-Cre* mice may be improved to some extent. These data also suggest that PHD2 inhibition may improve glucose metabolism in the presence of insulin resistance.

Phd2$^{f/f}$/aP2-Cre mice showed several beneficial morphological features of adipose tissue. First, the size of adipocytes in PHD2-deficient WAT was reduced. It is generally accepted that better glucose tolerance is associated with smaller adipocyte size and conversely that hypertrophied adipocytes are strongly linked to insulin resistance.[2] Second, macrophage infiltration into WAT was significantly suppressed in *Phd2$^{f/f}$/aP2-Cre* mice. Although the causal relationship might be difficult to determine, alteration of morphological features by *PHD2* deletion should cause better glucose tolerance and insulin sensitivity.

Although hypoxia has been known to reduce body weight[9] and fat mass,[26–28] it is intriguing that even PHD2 deletion in adipocytes showed a similar effect. In PHD2-deficient adipocytes, the glycolytic pathway becomes dominant because of the HIF-induced expression of glucose transporter and glycolytic enzymes, which is often called aerobic glycolysis.[29] Glycolysis is an inefficient way to produce energy compared with oxidative phosphorylation. Hence, the cells depending on glycolysis consume more glucose wastefully compared with those depending on oxidative phosphorylation when both cell types are required to generate an equal amount of ATP.[30] Therefore, PHD2-deficient adipocytes may consume more glucose than normal adipocytes. Although an in vitro study showed that PHD2 knockdown increases lactate production in the supernatant, the serum lactate level was rather decreased in *Phd2$^{f/f}$/aP2-Cre* mice. The reason for this discrepancy is not clear but may be due to a reduction in adiposity in *Phd2$^{f/f}$/aP2-Cre* mice. Because HFD loading increased serum lactate levels even in control mice (Table), the decrease in lactate levels in *Phd2$^{f/f}$/aP2-Cre* mice may reflect the reduced total adipose tissue mass.

PHD2 deletion attenuated fatty acid synthesis possibly through *Pdk1* upregulation. PDK1 suppresses the activity of pyruvate dehydrogenase, which catalyzes the conversion of pyruvate to acetyl CoA, an essential substrate for de novo fatty acid synthesis.[25] As a result, lipogenesis is expected to be reduced. In addition, *PHD2* deletion in adipocytes may enhance lipid consumption. *Phd2$^{f/f}$/aP2-Cre* mice consumed more oxygen with a lower respiratory exchange ratio and showed reduced lipid content in BAT, which may be explained, at least in part, by the upregulation of *Ucp1* expression. However, the detailed mechanism for UCP-1 upregulation is not clear at this point because UCP-1 is not a target gene of HIF. Overall, *PHD2* deletion–associated reprogramming of glucose and lipid metabolism might contribute to obesity resistance.

It is reported that hypoxia inhibits adipogenesis through upregulation of DEC1.[13] DEC1 is a transcription factor induced by HIF-1α that suppresses peroxisome proliferator–activated receptor-γ expression, resulting in the inhibition of adipogenesis. DEC1 expression in adipose tissue from *Phd2$^{f/f}$/aP2-Cre* mice was increased. However, peroxisome proliferator–activated receptor-γ expression is rather increased in WAT from *Phd2$^{f/f}$/aP2-Cre* mice (Figure 4A). Therefore, it is unlikely that DEC1 is involved in the reduced adiposity in *Phd2$^{f/f}$/aP2-Cre* mice.

Unexpectedly, we have found that Akt phosphorylation and Glut4 expression in the skeletal muscle of *Phd2$^{f/f}$/aP2-Cre* mice were increased. These data may suggest that insulin sensitivity is improved in HFD-fed *Phd2$^{f/f}$/aP2-Cre* mice compared with HFD-fed control mice. It is reported that Glut4 expression in skeletal muscle is suppressed in a rat model of insulin resistance,[31] suggesting that Glut4 upregulation in *Phd2$^{f/f}$/aP2-Cre* mice may be due to an improvement in insulin sensitivity. However, it is not clear how PHD2 deficiency in adipocytes affects the skeletal muscle insulin signaling pathway; further study is needed.

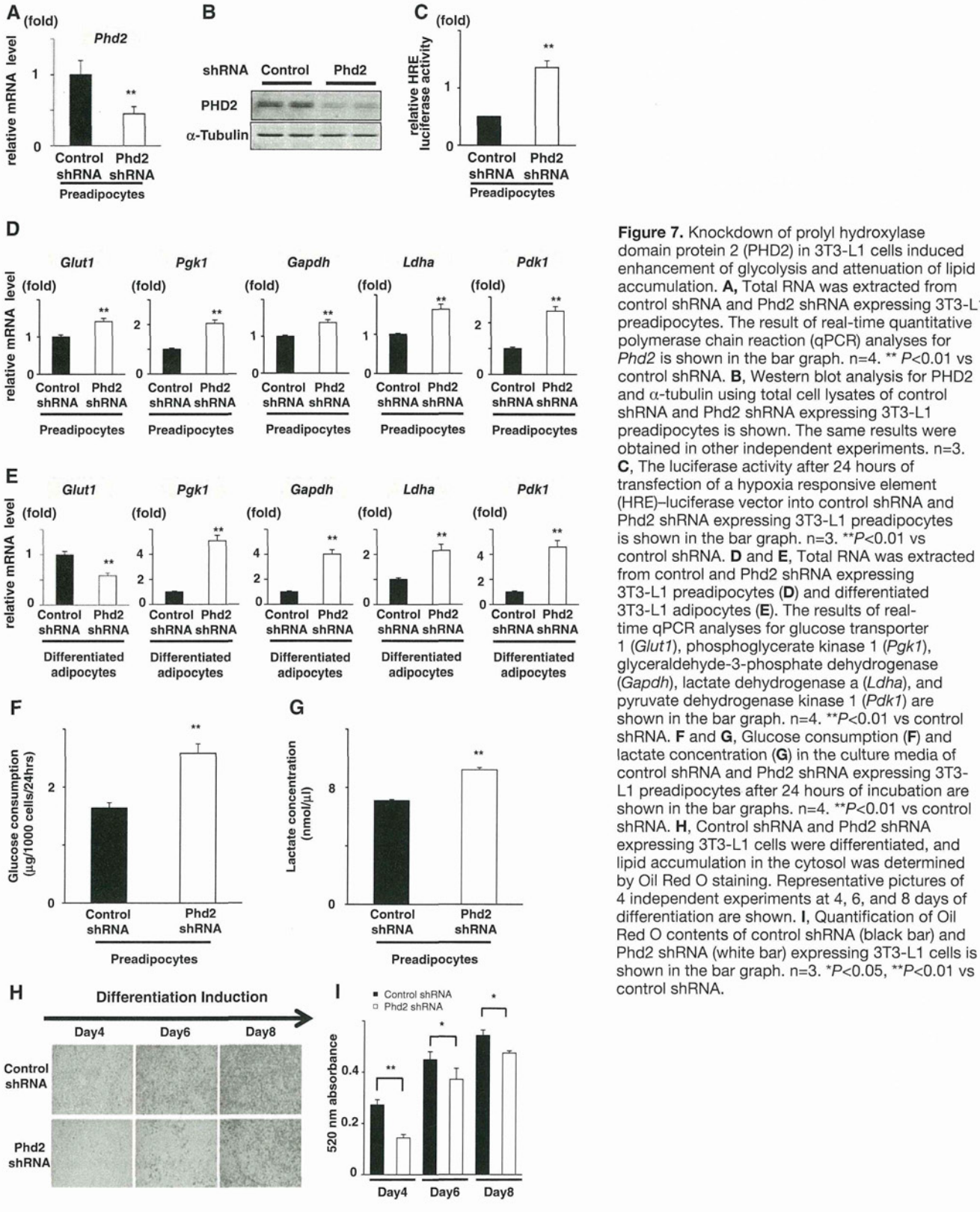

Figure 7. Knockdown of prolyl hydroxylase domain protein 2 (PHD2) in 3T3-L1 cells induced enhancement of glycolysis and attenuation of lipid accumulation. **A,** Total RNA was extracted from control shRNA and Phd2 shRNA expressing 3T3-L1 preadipocytes. The result of real-time quantitative polymerase chain reaction (qPCR) analyses for *Phd2* is shown in the bar graph. n=4. ** $P<0.01$ vs control shRNA. **B**, Western blot analysis for PHD2 and α-tubulin using total cell lysates of control shRNA and Phd2 shRNA expressing 3T3-L1 preadipocytes is shown. The same results were obtained in other independent experiments. n=3. **C**, The luciferase activity after 24 hours of transfection of a hypoxia responsive element (HRE)–luciferase vector into control shRNA and Phd2 shRNA expressing 3T3-L1 preadipocytes is shown in the bar graph. n=3. **$P<0.01$ vs control shRNA. **D** and **E**, Total RNA was extracted from control and Phd2 shRNA expressing 3T3-L1 preadipocytes (**D**) and differentiated 3T3-L1 adipocytes (**E**). The results of real-time qPCR analyses for glucose transporter 1 (*Glut1*), phosphoglycerate kinase 1 (*Pgk1*), glyceraldehyde-3-phosphate dehydrogenase (*Gapdh*), lactate dehydrogenase a (*Ldha*), and pyruvate dehydrogenase kinase 1 (*Pdk1*) are shown in the bar graph. n=4. **$P<0.01$ vs control shRNA. **F** and **G**, Glucose consumption (**F**) and lactate concentration (**G**) in the culture media of control shRNA and Phd2 shRNA expressing 3T3-L1 preadipocytes after 24 hours of incubation are shown in the bar graphs. n=4. **$P<0.01$ vs control shRNA. **H**, Control shRNA and Phd2 shRNA expressing 3T3-L1 cells were differentiated, and lipid accumulation in the cytosol was determined by Oil Red O staining. Representative pictures of 4 independent experiments at 4, 6, and 8 days of differentiation are shown. **I**, Quantification of Oil Red O contents of control shRNA (black bar) and Phd2 shRNA (white bar) expressing 3T3-L1 cells is shown in the bar graph. n=3. *$P<0.05$, **$P<0.01$ vs control shRNA.

It is known that adipose tissue in obese patients is subjected to hypoxia and HIF is accumulated,[32–34] which is explained by the facts that hypertrophied adipocytes become physically distant from capillaries and that inflammatory cells infiltrating into adipose tissue consume a substantial amount of oxygen. However, it has not been determined whether hypoxia in obese adipose tissue plays a causative role in obesity-associated metabolic abnormalities.[33,35] Recently, adipocyte-specific HIF-1α transgenic mice have been reported.[36] The transgenic mice gained more body weight than controls on both normal diet

and an HFD, showing glucose intolerance and insulin resistance. The adipose tissue in HIF-1α transgenic mice developed more fibrosis in association with local inflammation. These phenotypes are opposite of our observation. We observed that PHD2 deficiency with increased HIF-1α and HIF-2α neither led to adipocyte hypertrophy or local inflammation nor worsened HFD-induced obesity and glucose intolerance. The reason for this discrepancy is not immediately clear at this stage, but one of the differences between the previous study and our study is upregulation of HIF-2α in adipocytes in *Phd2$^{f/f}$/aP2-Cre* mice. Interestingly, HIF-1α and HIF-2α have opposite effects on adipogenesis: HIF-1α inhibits adipogenesis[13] and HIF-2α promotes it.[37] Therefore, the net effects by PHD2 inhibition on adipose tissue formation may be more complicated than the consequence of a single HIF-1α overexpression. Another possibility is that there may be unidentified substrates of PHD2 for hydroxylation that may be related to glucose and lipid metabolism and inflammation. In contrast, our observation is supported by several lines of evidence from genetically modified mice.[30,38,39] Overexpression of a dominant-negative form of HIF-1α in adipocytes accelerated HFD-induced glucose intolerance and insulin resistance and induced more severe obesity.[38] Another study showed that factor inhibiting HIF-1α–deficient mice that have elevated HIF activity are also resistant to HFD-induced body weight gain and glucose intolerance.[39] This evidence consistently suggests that HIF signaling is positively linked to resistance to obesity and associated metabolic abnormalities. It is of note that our study revealed that inhibition of PHD2 in adipocytes sufficiently attenuated HFD-induced glucose intolerance and obesity without an increase in serum lactate level, which is observed in SIRT6-deficient mice.[30] Therefore, inhibition of PHD in adipocytes might be meritorious in terms of clinical application.

The limitation of the present study is that we have not excluded the possible involvement of PHD2-deficient macrophages because the *aP2* gene is known to be expressed in not only adipocytes but also macrophages.[40] However, the reduction in PHD2 expression in bone marrow–derived macrophages or stromal vascular fraction that is rich in macrophages in *Phd2$^{f/f}$/aP2-Cre* mice was modest and not so remarkable compared with that in adipocytes. Therefore, the effect of PHD2-deletion in macrophages may play a relatively minor role in the reduction of fat mass and the improvement in glucose metabolism in *Phd2$^{f/f}$/aP2-Cre* mice.

Conclusions

We showed in this study that PHD2 in adipocytes plays a multifaceted role in the regulation of metabolism and inflammation in diet-induced obesity. Adipocyte-specific *Phd2* deletion ameliorates diet-induced obesity and several obesity-associated metabolic abnormalities. Thus, PHD2 in adipocytes may be a novel target for the treatment of patients with metabolic syndrome.

Acknowledgments

We acknowledge the technical expertise of the Support Center for Education and Research, Kyushu University.

Sources of Funding

This work was supported in part by a Grant-in-Aid for Scientific Research from the Ministry of Education, Culture, Sports, Science, and Technology of Japan (19590867 to Dr Ichiki) and research grant 2010 from AstraZeneca, SENSHIN Medical Research Foundation, Japanese Foundation for Applied Enzymology, and Takeda Medical Research Foundation to Dr Ichiki.

Disclosures

None.

References

1. Van Gaal LF, Mertens IL, De Block CE. Mechanisms linking obesity with cardiovascular disease. *Nature*. 2006;444:875–880.
2. Hotamisligil GS. Inflammation and metabolic disorders. *Nature*. 2006;444:860–867.
3. Martínez JA. Mitochondrial oxidative stress and inflammation: an slalom to obesity and insulin resistance. *J Physiol Biochem*. 2006;62:303–306.
4. Ozcan U, Cao Q, Yilmaz E, Lee AH, Iwakoshi NN, Ozdelen E, Tuncman G, Görgün C, Glimcher LH, Hotamisligil GS. Endoplasmic reticulum stress links obesity, insulin action, and type 2 diabetes. *Science*. 2004;306:457–461.
5. Nishimura S, Manabe I, Nagasaki M, Eto K, Yamashita H, Ohsugi M, Otsu M, Hara K, Ueki K, Sugiura S, Yoshimura K, Kadowaki T, Nagai R. CD8+ effector T cells contribute to macrophage recruitment and adipose tissue inflammation in obesity. *Nat Med*. 2009;15:914–920.
6. Cooke D, Bloom S. The obesity pipeline: current strategies in the development of anti-obesity drugs. *Nat Rev Drug Discov*. 2006;5:919–931.
7. Després JP, Golay A, Sjöström L; Rimonabant in Obesity-Lipids Study Group. Effects of rimonabant on metabolic risk factors in overweight patients with dyslipidemia. *N Engl J Med*. 2005;353:2121–2134.
8. Christensen R, Kristensen PK, Bartels EM, Bliddal H, Astrup A. Efficacy and safety of the weight-loss drug rimonabant: a meta-analysis of randomised trials. *Lancet*. 2007;370:1706–1713.
9. Shukla V, Singh SN, Vats P, Singh VK, Singh SB, Banerjee PK. Ghrelin and leptin levels of sojourners and acclimatized lowlanders at high altitude. *Nutr Neurosci*. 2005;8:161–165.
10. Allahdadi KJ, Walker BR, Kanagy NL. Augmented endothelin vasoconstriction in intermittent hypoxia-induced hypertension. *Hypertension*. 2005;45:705–709.
11. Simler N, Grosfeld A, Peinnequin A, Guerre-Millo M, Bigard AX. Leptin receptor-deficient obese Zucker rats reduce their food intake in response to hypobaric hypoxia. *Am J Physiol Endocrinol Metab*. 2006;290:E591–E597.
12. Quintero P, Milagro FI, Campión J, Martínez JA. Impact of oxygen availability on body weight management. *Med Hypotheses*. 2010;74:901–907.
13. Yun Z, Maecker HL, Johnson RS, Giaccia AJ. Inhibition of PPAR gamma 2 gene expression by the HIF-1-regulated gene DEC1/Stra13: a mechanism for regulation of adipogenesis by hypoxia. *Dev Cell*. 2002;2:331–341.
14. Kaelin WG Jr, Ratcliffe PJ. Oxygen sensing by metazoans: the central role of the HIF hydroxylase pathway. *Mol Cell*. 2008;30:393–402.
15. Semenza GL, Roth PH, Fang HM, Wang GL. Transcriptional regulation of genes encoding glycolytic enzymes by hypoxia-inducible factor 1. *J Biol Chem*. 1994;269:23757–23763.
16. Semenza GL, Jiang BH, Leung SW, Passantino R, Concordet JP, Maire P, Giallongo A. Hypoxia response elements in the aldolase A, enolase 1, and lactate dehydrogenase A gene promoters contain essential binding sites for hypoxia-inducible factor 1. *J Biol Chem*. 1996;271:32529–32537.
17. Kim JW, Tchernyshyov I, Semenza GL, Dang CV. HIF-1-mediated expression of pyruvate dehydrogenase kinase: a metabolic switch required for cellular adaptation to hypoxia. *Cell Metab*. 2006;3:177–185.
18. Papandreou I, Cairns RA, Fontana L, Lim AL, Denko NC. HIF-1 mediates adaptation to hypoxia by actively downregulating mitochondrial oxygen consumption. *Cell Metab*. 2006;3:187–197.
19. Fraisl P, Aragonés J, Carmeliet P. Inhibition of oxygen sensors as a therapeutic strategy for ischaemic and inflammatory disease. *Nat Rev Drug Discov*. 2009;8:139–152.
20. Berra E, Benizri E, Ginouvès A, Volmat V, Roux D, Pouysségur J. HIF prolyl-hydroxylase 2 is the key oxygen sensor setting low steady-state levels of HIF-1alpha in normoxia. *EMBO J*. 2003;22:4082–4090.
21. Takeda K, Ho VC, Takeda H, Duan LJ, Nagy A, Fong GH. Placental but not heart defects are associated with elevated hypoxia-inducible factor

alpha levels in mice lacking prolyl hydroxylase domain protein 2. *Mol Cell Biol*. 2006;26:8336–8346.
22. Nishimura S, Manabe I, Nagasaki M, Hosoya Y, Yamashita H, Fujita H, Ohsugi M, Tobe K, Kadowaki T, Nagai R, Sugiura S. Adipogenesis in obesity requires close interplay between differentiating adipocytes, stromal cells, and blood vessels. *Diabetes*. 2007;56:1517–1526.
23. Weisberg SP, McCann D, Desai M, Rosenbaum M, Leibel RL, Ferrante AW Jr. Obesity is associated with macrophage accumulation in adipose tissue. *J Clin Invest*. 2003;112:1796–1808.
24. Xu H, Barnes GT, Yang Q, Tan G, Yang D, Chou CJ, Sole J, Nichols A, Ross JS, Tartaglia LA, Chen H. Chronic inflammation in fat plays a crucial role in the development of obesity-related insulin resistance. *J Clin Invest*. 2003;112:1821–1830.
25. Lum JJ, Bui T, Gruber M, Gordan JD, DeBerardinis RJ, Covello KL, Simon MC, Thompson CB. The transcription factor HIF-1alpha plays a critical role in the growth factor-dependent regulation of both aerobic and anaerobic glycolysis. *Genes Dev*. 2007;21:1037–1049.
26. Westerterp KR, Kayser B, Wouters L, Le Trong JL, Richalet JP. Energy balance at high altitude of 6,542 m. *J Appl Physiol*. 1994;77:862–866.
27. Westerterp-Plantenga MS, Westerterp KR, Rubbens M, Verwegen CR, Richelet JP, Gardette B. Appetite at "high altitude" [Operation Everest III (Comex-'97)]: a simulated ascent of Mount Everest. *J Appl Physiol*. 1999;87:391–399.
28. Reynolds RD, Lickteig JA, Deuster PA, Howard MP, Conway JM, Pietersma A, deStoppelaar J, Deurenberg P. Energy metabolism increases and regional body fat decreases while regional muscle mass is spared in humans climbing Mt. Everest. *J Nutr*. 1999;129:1307–1314.
29. Gatenby RA, Gillies RJ. Why do cancers have high aerobic glycolysis? *Nat Rev Cancer*. 2004;4:891–899.
30. Zhong L, D'Urso A, Toiber D, Sebastian C, Henry RE, Vadysirisack DD, Guimaraes A, Marinelli B, Wikstrom JD, Nir T, Clish CB, Vaitheesvaran B, Iliopoulos O, Kurland I, Dor Y, Weissleder R, Shirihai OS, Ellisen LW, Espinosa JM, Mostoslavsky R. The histone deacetylase Sirt6 regulates glucose homeostasis via Hif1alpha. *Cell*. 2010;140:280–293.
31. Leguisamo NM, Lehnen AM, Machado UF, Okamoto MM, Markoski MM, Pinto GH, Schaan BD. GLUT4 content decreases along with insulin resistance and high levels of inflammatory markers in rats with metabolic syndrome. *Cardiovasc Diabetol*. 2012;11:100.
32. Ye J. Emerging role of adipose tissue hypoxia in obesity and insulin resistance. *Int J Obes (Lond)*. 2009;33:54–66.
33. Yin J, Gao Z, He Q, Zhou D, Guo Z, Ye J. Role of hypoxia in obesity-induced disorders of glucose and lipid metabolism in adipose tissue. *Am J Physiol Endocrinol Metab*. 2009;296:E333–E342.
34. Hosogai N, Fukuhara A, Oshima K, Miyata Y, Tanaka S, Segawa K, Furukawa S, Tochino Y, Komuro R, Matsuda M, Shimomura I. Adipose tissue hypoxia in obesity and its impact on adipocytokine dysregulation. *Diabetes*. 2007;56:901–911.
35. Trayhurn P, Wang B, Wood IS. Hypoxia in adipose tissue: a basis for the dysregulation of tissue function in obesity? *Br J Nutr*. 2008;100:227–235.
36. Halberg N, Khan T, Trujillo ME, Wernstedt-Asterholm I, Attie AD, Sherwani S, Wang ZV, Landskroner-Eiger S, Dineen S, Magalang UJ, Brekken RA, Scherer PE. Hypoxia-inducible factor 1alpha induces fibrosis and insulin resistance in white adipose tissue. *Mol Cell Biol*. 2009;29:4467–4483.
37. Shimba S, Wada T, Hara S, Tezuka M. EPAS1 promotes adipose differentiation in 3T3-L1 cells. *J Biol Chem*. 2004;279:40946–40953.
38. Zhang X, Lam KS, Ye H, Chung SK, Zhou M, Wang Y, Xu A. Adipose tissue-specific inhibition of hypoxia-inducible factor 1{alpha} induces obesity and glucose intolerance by impeding energy expenditure in mice. *J Biol Chem*. 2010;285:32869–32877.
39. Zhang N, Fu Z, Linke S, Chicher J, Gorman JJ, Visk D, Haddad GG, Poellinger L, Peet DJ, Powell F, Johnson RS. The asparaginyl hydroxylase factor inhibiting HIF-1alpha is an essential regulator of metabolism. *Cell Metab*. 2010;11:364–378.
40. Furuhashi M, Hotamisligil GS. Fatty acid-binding proteins: role in metabolic diseases and potential as drug targets. *Nat Rev Drug Discov*. 2008;7:489–503.

CLINICAL PERSPECTIVE

Obesity is associated with low-grade chronic inflammation, dysregulated adipocytokine production, and increased oxidative stress in visceral adipose tissue, which is believed to result in insulin resistance, high blood pressure, and acceleration of atherosclerosis. Although hypoxia has long been known to reduce body weight in both humans and animals, the role of the hypoxia response system, including hypoxia-inducible factor and an oxygen sensor, prolyl hydroxylase domain protein (PHD), in the regulation of fat mass and glucose metabolism remains controversial. Therefore, in the present study, we sought to determine whether deletion of PHD2, a main isoform of PHD, in adipose tissue affects high-fat diet–induced obesity and glucose intolerance. We showed that PHD2 deficiency in adipocyte resulted in upregulation of hypoxia-inducible factor and attenuated high-fat diet–induced body weight gain and glucose intolerance compared with control mice. These effects seemed to be mediated by upregulation of glycolytic enzymes in white adipose tissue and uncoupling protein-1 in brown adipose tissue in the PHD2-deficient mice. The PHD2-deficient mice also showed modest improvement in insulin sensitivity. The improvement in glucose metabolism is associated with a decrease in adipocyte size, macrophage infiltration, and abnormal angiogenesis of white adipose tissue in the PHD2-deficient mice. Because of the worldwide pandemic of obesity and diabetes mellitus, a novel strategy that is effective for the treatment of both conditions has been sought. The present study suggests that PHD2 inhibition in adipocyte may be a new therapeutic approach to reduce body weight and to improve glucose tolerance simultaneously.

SUPPLEMENTAL MATERIAL

Supplemental File for Supplemental Methods, Supplemental Tables, Supplemental Figures (1-4) and Legends for Supplemental Figures.

Supplemental Methods

Materials

Dulbecco's Modified Eagle Medium (DMEM) was purchased from GIBCO BRL-Invitrogen Co. (Carlsbad, CA, U.S.A.). Fetal bovine serum (FBS) was purchased from SAFC Biosciences Inc. (Lenexa, KS, U.S.A.). A mouse monoclonal anti-α-tubulin antibody was purchased from Sigma-Aldrich Co. (St. Louis, MO, U.S.A.). Horseradish peroxidase-conjugated secondary antibodies (anti-rabbit and anti-mouse IgG) were purchased from Vector Laboratories, Inc. (Burlingame, CA, U.S.A.). Luciferase assay system was purchased from Promega Co. (Madison, WI, U.S.A.). Other chemical reagents were purchased from Wako Pure Chemical Industries, Ltd. (Osaka, Japan) unless otherwise stated.

Generation of adipocyte-specific PHD2-deficient mice.

To knockout *Phd2* gene in adipocytes, previously generated *Phd2*-floxed mice were used ($Phd2^{f/+}$).[1] Transgenic mice expressing Cre recombinase under control of *aP2* gene promoter (*aP2-Cre*) were purchased from the Jackson Laboratory (Stock Number 5069, Bar Harbor, Maine). $Phd2^{f/+}$ mice were crossed with *aP2-Cre* mice to obtain $Phd2^{f/+}$/*aP2-Cre* mice. Then, mice with PHD2 deletion in adipocyte ($Phd2^{f/f}$/*aP2-Cre*) were generated by stepwise crossing of $Phd2^{f/+}$/*aP2-Cre* mice with $Phd2^{f/f}$ mice. $Phd2^{f/f}$ mice were served as controls. The primers to detect *Phd2*-floxed gene and *Cre* gene were previously described.[2] These mice were fed a

high-fat diet (HFD) containing 60% kcal fat (High Fat Diet 32, Clea Japan) from 12 weeks to 18 weeks. Mice at the age of 12- and 18-week-old were analyzed. All procedures were approved by Animal Care and Use Committee, Kyushu University and conducted in accordance with the institutional guidelines.

Histological analysis

Adipose tissues were fixed in 10% neutral buffered formaldehyde solution overnight and embedded in paraffin. Paraffin sections were stained with hematoxylin and eosin (H&E). Ten images of H&E stained sections were acquired from each animal and cross-sectional area of each adipocyte was determined using the software Dynamic cell count BZ-HIC (Keyence, Japan). To detect macrophage infiltration, the paraffin sections were immunohistochemically stained with an anti-mouse Mac-3 antibody (Santa Cruz Biotechnology, Inc., Santa Cruz, CA) and detected with DAB chromogen. For morphological analysis of blood vessels, adipose tissues were minced with scissors to small pieces (1~2 mm) and the tissues were directly stained with FITC-Conjugate *Bandeiraea simplicifolia* lectin (Sigma Sigma-Aldrich Co., St. Louis, MO, U.S.A.) for two hours at room temperature. Then, the tissues were counterstained with 4',6-diamino-2-phenylindole (DAPI) and examined using the confocal laser scanning microscope A1R (Nikon, Japan). Capillary density was determined by counting blood vessels intersecting 1 mm line drawn in the photos of lectin-stained adipose tissues.

Glucose tolerance test and insulin tolerance test

Mice were starved for 6 hours.[3] For glucose tolerance test, mice were injected intraperitoneally with glucose (1 g/kg of body weight). For insulin tolerance test, mice were injected intraperitoneally with rapid insulin (0.5 IU/kg of body weight). Blood sample was taken from tail

vein at various time points and blood glucose concentrations were determined by using Glutest Every (Sanwa Kagaku Kenkyusho, Japan).

Measurement of serum levels of triglyceride, cholesterol, insulin, lactate and cytokines.

Serum triglyceride and total cholesterol levels were determined by commercially available kits, Triglyceride E-test Wako (Wako) and Cholesterol E-test Wako (Wako), respectively. Serum insulin levels were determined by insulin ELISA kit (Morinaga Institute of Biological Science, Japan). Serum lactate level was determined by lactate assay kit (BioVision, Mountain View, CA). Serum cytokine levels were determined by ELISA kits (R&D systems Inc. Minneapolis, MN, USA).

Western blot analysis

Protein preparation and Western blot analysis for PHD2,[1] HIF-1α, HIF-2α (Novus Biologicals, Littleton, CO USA), lactate dehydrogenase (LDH) a, Glut 4, Akt and phospho-Akt (Cell Signaling Technology, Danvers, MA, USA) were performed as described previously.[2] α-tubulin (Sigma-Aldrich Co.) or cyclic AMP response element binding protein (CREB, Cell Signaling Technology) was used as a loading control.

Isolation of adipocyte-enriched fraction and stromal vascular fraction (SVF) from white adipose tissues (WAT)

The epididymal fat tissue was minced and digested with collagenase (3 mg/ml, Sigma) in phosphate-buffered saline supplemented with bovine serum albumin (2%, Sigma) at 37 °C for 60 minutes with gentle agitation. Then, the digested fat tissues were filtered through a 250 μm nylon mesh and centrifuged at 430 g for 1 minutes. The sediments were used as a SVF and floating